

Effective elastic properties of randomly distributed void models for porous materials

B. Li, B. Wang and S.R. Reid

School of Engineering, College of Physical Science, University of Aberdeen, UK

ABSTRACT

Many 2D analytical models are available for analysis of the effective elastic properties of porous materials. Most of these models adopt circular voids of a uniform diameter in superlattice arrays, such as unit void or periodically positioned models. There are two issues in a realistic representation of porous materials: the random distribution of a statistically sufficiently large number of voids in the model, and the random distribution of the size and position of the voids. Numerical schemes such as FEM or BEM approaches have also been presented to cater for regular patterned circular voids. However, due to the large number of elements needed to produce a sufficient accuracy for curved boundary of circular voids, modelling of a statistically sufficient number of voids with a random distribution in both the void size and the has yet been seen.

Modelling based on a FEM approach using a simplified approximation in void geometry is proposed here for the calculation of effective elastic properties of porous solids. A

plane strain configuration of a square geometry is adopted for the voids. This simplified square shape allows for a large number of voids to be simulated with a random distribution for both void *sizes* and their *locations*. The problem of anisotropy, which arises from the square shape, is discussed. It is verified that along the two main axial directions (parallel to the sides of the square voids), elastic properties remain the same as predicted by those using a circular void geometry. This square-shaped approximation, with its reduced requirement on FE analysis, has the potential to be extended to 3-dimensional modelling for a realistic simulation of engineering materials.

Key words: porous material, elastic properties, finite element modelling, random distribution

1. Introduction

A number of micro-mechanics models have been proposed to estimate the effective elastic properties of materials with inclusions, such as voids and micro-cracks. Many monographs, including those by Christensen [1], Mura [2], Taya and Arsenault [3], Huang et al [4], etc., covered most of the development in this area up to 1990s. Most of the research was of theoretical approach of various kinds. Only few data was obtained from experiments or numerical simulations. Several types of periodically positioned arrays of circular voids of a uniform diameter were considered by Isida and Igawa [5], and Day [6]. But the efficiency and accuracy of these models have not been critically evaluated.

It is well understood that the elastic properties of porous materials are not sensitive to the voids' shape [11], but are much dependent on the number and size of the voids. The location distribution of the voids is another factor. Fig. 1 shows the optical micrograph of sections of bronze samples with the porosity of 17%, 29% and 39%, respectively. The samples were made from a sintering process using powders of bronze with 10% tin (Wt%) [12]. The micro textures show a certain degree of non-uniformity in both the pore size and the position. Large pores on average of 100 ~ 200 micron are isolated, and there appears some regions of segregation or clustering of pores. For such materials which contain a large quantity of defects, debris and voids of irregular shapes, sizes and locations, one would inevitably ask the question on how suitable the unit cell approach can be. It appears the unit cell or periodic models are more appropriate for cellular materials of a much more regular morphology, such as honeycombs.

With previous knowledge in mind, the main objective of this work is to develop a numerical model for porous materials, containing random features in both the size and the position of voids, probably by using a reasonably simple but statistically representative description, say, a Guassing normal distribution [14]. A consideration of such a system is probably close to the best we can get in terms of modelling a realistic material containing natural defects. This would also allow the existing theoretical schemes to be evaluated and compared, and possibly be extended for a wider scope, such as for modelling in 3D.

In almost all previous models, voids are approximated as perfectly circular voids of a uniform diameter. While there are good reasons for this – mainly for the benefit of simpler mathematical formulations in analytical approaches, it poses a significant challenge for numerical modelling of a large number of voids with random geometric features. The fine meshes needed in a numerical scheme, such as a finite element model, to cater for the curved boundary of circular voids lead to the total element number required so high that even for 2D modelling, calculations become extremely expensive if not prohibitive. To overcome this problem so that the random geometric features of the voids can be addressed, we adopt a much simpler geometry of the voids by using a square shape, with all the square voids aligned in parallel, i.e., of the same axial directions (see Fig. 3). This choice is governed by the observation that materials elastic properties are less sensitive to the shape of the voids [11]. The simplified void shape allows for a simpler mesh to be used. Though this model will introduce singularity at the void corners and anisotropy (orthotropy) due to the directional feature of the square voids, it will be shown later in this paper that the effective elastic properties are not affected in the axial directions parallel to the sides of the square shape, thus providing an effective and efficient approach for simulation.

This paper is arranged in the following way. The square void model is introduced with the inclusion of a normal distribution for both the size and position of the voids. One key issue is the test to find out the “minimum” number of voids needed to produce stabilised results, i.e. convergence. This is followed by a discussion on issues of anisotropy, and the effect of the mean and the standard deviation of a normal distribution. Finally, the

outcome of the calculation is then compared with some well known models to assess the validity and efficiency. A comparison with the experiments on sintered porous metals is also provided.

2. A 2D double normal distribution model for the void size and position

Let's consider a plate in which there are randomly distributed voids of a square shape. A normal distribution function is first selected, for instance, for the position of the voids as a random parameter:

$$y = \frac{1}{\sqrt{2\pi} \cdot \sigma} e^{-\frac{(x-\mu)^2}{2\sigma^2}} \times S_h \quad (1)$$

where x represents the shortest distance between the centres of the neighbouring voids, y is the probability density of the voids whose shortest distance with other voids is x . S_h is a constant used to obtain a specified porosity. σ and μ are the normal distribution parameters in which σ is the standard deviation of the shortest distance between the centres of the voids, describing the shape of the normal distribution function; μ is the average (mean) shortest distance between the centres of voids, and should be large than the side length of any square voids. A normal density function is shown in Fig 2. To obtain the number of voids whose shortest distance amongst them is a random parameter, as denoted by x here, the area below the normal density function curve in Fig. 2 is divided into columns of equally width. The columns provide the number of voids corresponding to their relative positions following the normal distribution. The parameter

S_h (common to all columns) is introduced as a factor to adjust the total number of voids in the model so that the porosity of the plate is kept at a specified value.

While the position distribution of the voids has been considered, Eq. (1) can also be used to determine the size distribution of the voids as a random parameter by replacing x as the void side length with μ being the average of side length. Fig. 2 can again be divided into equal columns to determine the number of voids in each size group.

The combination of the two distributions, i.e. a double normal distribution with one for the void position and the other for the void size provides a pseudo model for realistic porous materials which can be built reasonably straightforward using the square void model proposed here. Fig. 3 shows an example of the outcome of this double normal distribution, where the variation in both the location and the size of the square voids in a unit plate are clearly illustrated. It shows an example of a unit plate of side length 100 with a porosity of 40%. A programme was written in a mathematical tool Mathcad [7] to generate the distributions, and a graphic tool AutoCAD [8] was used to produce the images. There are 444 square voids in total with an average side length 3.0 and a mean shortest distance of 3.5 among them.

ABAQUS 6.7 [9] was then used as the solver, and the 4-node bilinear plane-stress element CP4S was chosen. The auto-meshing function provided by the code was selected with 1000 divisions in each border line of the plate. Fine grids of elements generated can be seen in Fig. 3. A simple uniaxial tension was applied using a uniformly distributed

loading (far field stress) in direction 2 with no constraints on the top and bottom boundaries in direction 1. The two boundaries on the sides are kept as free boundaries. Only the elastic response is assumed, from which the effective elastic properties are calculated.

2.1 Convergence of the model

Due to the random nature of the normal distribution, one can have a different distribution with the same μ and σ each time a distribution is generated. It needs to be checked that the FE models based on different distributions of the same μ and σ lead to agreeable results – i.e. a convergence of the simulation. In this study, each case is run three times by using three randomly generated distributions with the same μ and σ . This allows the results to be checked for their agreeability.

Another issue is the minimum number of voids needed for each model. When the porosity of the model is pre-selected as the controlling factor, the total number of voids becomes dependent on the average size of the voids. For instance, a choice of larger sized voids leads to a fewer numbers of voids, and vice versa.

Fig. 4 shows the results of simulations carried out on a the plate of the size 100 by 100 under uniaxial tension loading in direction 2. Four different μ - the average size of the voids size, were simulated while σ was kept constant. Note that μ represents the mean of the normal distribution, and σ , the standard deviation, determines the shape of the

normal distribution of the void size. Three repeated runs were carried out for each pair of μ and σ . Fig. 4(a) to e) shows the calculated effective Young's modulus for different porosities. The values in the brackets of the horizontal axes give the numbers of voids in the model corresponding to the average void size for the porosity specified. For instance, in Fig. 4(a), 222 voids are used (needed) with the average void size being 3; 56 voids are needed when the average size is 6.

Fig. 4 also illustrates that a larger number of small voids generally give a more converged result. For instance, the differences between the 3 runs are at the least for the average size being 3 (high total void number), but at the largest for the average size being 6 (low total void number). There is conformity of this trend in all cases of porosities. This apparently indicates that there is advisable to maintain a minimum number of voids in the model in order to achieve better statistical stability (convergence). Based on this, it was decided that the void size of 3 being chosen for most of the calculations.

2.2 Anisotropy

Due to the square shape of the voids in parallel orientations, it generates two major perpendicular axes. This may lead the properties to become directional, probably orthotropic. Whereas in the case of circular voids, the properties are understood to be isotropic. To evaluate this, the effective shear modulus G was studied. For an isotropic solid, the modulus can be calculated from the Young's modulus E and the Poisson ratio ν .

$$G = E/2(1+\nu) \quad (2)$$

where E and ν are obtained from a simple tension case.

Alternatively, a pure shear loading model can be used to obtain the value of shear modulus G . If the model is isotropic, the values of G from the two methods should be the same, or numerically close to each other. A large difference, however, would indicate a non isotropic nature. Fig. 5 illustrates the results of the simulated effective shear modulus from simulations of three different loading cases. Apart from the uniaxial tensile one as discussed previously, a biaxial tensile case is included where equal uniform stresses were applied in both directions 1 and 2, from which G was calculated from Eqn. (2). The legend label “Pure shear” indicates the results from the simulation of a pure shear model where equal shear stress was applied on all sides of the plate. There is a clear difference between the modulus obtained from the pure shear model and those obtained from the uniaxial and biaxial loading cases, suggesting that it is anisotropic. Actually, the close agreement between the uniaxial and biaxial loading cases shows that the square void model is orthogonal.

On the other hand, the agreement of the calculated effective elastic modulus to those of existing theoretical and numerical models (e.g. [5-6], [10]), as to be discussed later in Figs. 9 and 10, suggests that although the square void is orthogonal, the properties along the two major axes are of the same as those from isotropic models. Therefore this square void model can be used to estimate the properties of general engineering materials with

voids of a random nature, as long as only the properties along the two major axes of the square void model are considered.

2.3 The influence of the mean μ and the standard deviation σ

A normal distribution has only two controlling parameters, the mean μ and the standard deviation σ . They represent different morphological features of the porous model. Their influence is studied here.

First, the void size length is fixed at 3 while the statistic features μ and σ are introduced for void positions, as shown in Figs. 6 and 7 for material porosities 30% and 40%. In Fig. 6, while the standard deviation σ of the void position is kept, for instance, at 0.2, the average shortest distance μ between the neighboring voids is changed for three different values as being 3.3, 3.4 and 3.5. Note that μ , as the shortest distance between the neighboring voids, needs to be bigger than the void size, ie. 3, but cannot be too big than 3. Three runs were carried out for each case. The results reveal an increase in the relative Young's modulus while the average shortest distance between voids increases. This can be easily understood since a larger average shortest distance between voids gives larger bridges between voids therefore stronger loading capacity, thus making the material harder to deform.

In Fig. 7, while the average shortest distance μ between the neighboring voids is kept constant at 3.3, the standard deviation σ of the shortest distance is changed to 0.12, 0.2

and 0.25. As in previous cases, the effective Young's modulus is shown for different porosities, and three runs of the distribution were carried out for each case. It can be seen that the average of the three runs does not change much, indicating that the effect of different σ is rather limited, probably negligible.

Furthermore, the random nature of the void size is investigated. Here the void side length μ is set to 3.0 and its standard deviation taken as 0.15, 0.2 and 0.25, respectively, while the average shortest distance between voids is kept at 3.2. The effective Young's modulus is shown in Fig. 8 for porosities of 30% and 40%. As in all previous cases, three runs were carried out for each distribution. The results shows limited effect, indicating the standard deviation is not a strongly influential factor.

3 Comparison with existing models

In Fig. 9, the present numerical results are compared with the theoretical solutions derived by Isida and Igawa [5]. They analyzed the zigzag positioned array of circular voids with a uniform diameter under uniaxial tension by assuming complex stress potentials, in the form of Laurent series expansions, to determine the unknown coefficients from the boundary conditions. They established the power series fitted to the results of effective Young's modulus, with respect to the change of volume fraction and a dimensionless parameter δ which concerns about the position distribution of voids array.

The results from two obtained power series for square ($\delta=1$) and triangular ($\delta=1/\sqrt{3}$) position arrays are used here.

Results of three distinct position arrays studied by Day et al [6] are also employed for comparison. The three curves in the figure correspond to those three cases circular voids of a uniform diameter a) periodically centred on a honeycomb lattice, b) periodically centred on a triangular lattice, and c) random centred. There is no overlapping between circles in the first two cases. In case c), there is no restriction on the circles overlapping.

By plotting the results from this study, using square shaped voids with a double normal distribution in both the size and the position, it can be observed that they all located between the curves of the triangular and square positioned arrays of circle voids of a uniform diameter obtained by Isida and Igawa [5]. However, the curves of hexagonal and triangular positioned arrays generated by Day et al [6] are slightly higher than the current results in general. The results for randomly overlapped superlattices are comparably much lower than all the other solutions.

Probably a more relevant comparison is illustrated in Fig. 10 to the results of Hu et al [10] in a boundary element modelling in which they studied normally distributed circular voids of uniform diameter. It can be seen that the two curves are very close to each other, which confirms that the square voids can be used for elastic properties. It needs to be pointed out that although the random feature of the void position was considered by Hu et al [10], they only considered circular voids of a uniform diameter. The addition of the

random variation in the void size in this study is a clear improvement. In fact, the benefit of using square shaped voids is much more significant – it provides a much simpler model in finite element analysis, paving the potential to be expanded to 3D.

The experimental results of the relative Young's modulus from Ref. [13] on sintered bronze samples from 18 to 39% porosities are also given in Fig. 10. Tests were carried out in simple compression modes on cylindrical samples under both quasi-static and dynamics loading conditions under various strain rates. It shows that the elastic properties are not sensitive to strain rate and confirms the good estimates provided by the present square shaped void model.

4. Conclusion and discussion

As an effort to bring modeling closer to realistic engineering materials, a double random distribution in void size and position is introduced in a finite element model to calculate the elastic properties of porous materials. This is found that in order to maintain a repeatable accuracy, a large number of voids are needed. This argument is shared by others [10]. As a consequence, modeling becomes prohibitively expensive. A square shaped void approach is therefore introduced in an effort to reduce the load of numerical work. Demonstrated in a 2D model, it has shown to be accurate for the elastic properties in the major axes of the square shape with good agreement to the available theoretical and numerical works, and test results.

The simplified void geometry also opens up the possibility for a three dimensional modeling with statistic features in the void size and position as a true reflection of the engineering materials with voids. This is yet to be done. Though the demand for the numerical capacity for such a 3D model cannot be under-estimated, only the simplified geometry, as a verified approximation, may make it possible.

Acknowledgement

The first author BL would like to acknowledge University of Aberdeen for partial funding to support his study.

References

1. R. Christensen, *Mechanics of Composite Materials*, John Wiley & Sons, New York, 1979
2. T. Mura, *Micromechanics of Defects in Solids*, Martinus Nijhoff Publisher, 1982.
3. M. Taya and R.J. Arsenault, *Metal Matrix Composites*, Pergamon Press, 1989.
4. Y. Huang, K.X. Hu, X. Weu and A. Chandra, A generalised self-consistent mechanics method for composite materials with multiphase inclusion, *Journal of Mechanics and Physics of Solids*, 42, 491-504, 1994.
5. M. Isida and H. Igawa, Analysis of zig-zag array of circular voids in an infinite solid under uniaxial tension, *International Journal of Solids and Structures*, 27, 849-864, 1992.

6. A.R. Day, K.A. Snyder, E.J. Garbanzo and M.F. Thorpe, The elastic module of a sheet containing circular voids, *Journal of Mechanics and Physics of Solids*, 40, 1031-1051, 1992.
7. Mathcad 14, PTC Worldwide Headquarters, 140 Kendrick Street, Needham, Massachusetts, 2007
8. AutoCAD, Autodesk, San Rafael, California, 2007
9. ABAQUS Manual, 6.7, HKS Inc., Providence, Rhode Island, 2007.
10. N. Hu, B. Wang, G.W. Tan, Z.H. Yao and W.F. Yuan, Effective elastic properties of 2D solids with circular voids: numerical simulations, *Composites Science and Technology*, 60, 1811-1823, 2000.
11. Cellular solids, 2nd Edition, Gibson and Ashby, Cambridge University Press, 1997
12. B. Wang, J. Zhang and G. Lu, Taylor impact tests for ductile porous materials - Part 2: Experiments, *International Journal of Impact Engineering*, Vol. 28, pp. 499-511, 2003.
13. B. Wang, J.R. Klepaczko, G. Lu and L.X. Kong, Viscoplastic behaviour of porous bronzes and irons, *Journal of Materials Processing Technology*, Vol. 113, pp. 574-580, 2001
14. Probability & Statistics for Engineers nad Scientists, 8th Edition, Walpole, Mayers, Mayers and Ye, Pearson, 2007

Captions of figures

Fig. 1 Micrograph (x50) of symmetric vertical sections of sintered bronze samples with porosity of (a) 17%, (b) 29% and (c) 39%.

Fig. 2 A normal distribution representing the void size and position. x is a physical parameter which can be, for instance, the minimum distance between the centres of the neighbouring voids, or the size (side length) of the void. y represents the probability density as in a normal distribution.

Fig. 3 A FE model with a double normal distribution (for void size and position) for a porous plate of 40% porosity

Fig. 4 Effective Young's modulus calculated for different porosities (a) 20%, (b) 30%, (c) 40%, (d) 50%, (e) 55%. Different void side lengths are used. Bracket shows the number of elements in the model.

Fig. 5 Effective shear modulus vs. porosity from different loading conditions. "Pure shear" indicates a pure shear model, while the shear modulus for the other two were calculated from the value of E and ν obtained from a uniaxial and a bi-axial tension modes, respectively.

Fig. 6 Effective Young's modulus vs. the mean of the average shortest distance between the centres of the neighboring voids. $\sigma = 0.2$ for the normal distribution and the void size is 3. Material porosities are (a) 30% and (b) 40%.

Fig. 7 Effective Young's modulus vs. the standard deviation σ of the normal distribution in the average shortest distance between the centres of the neighboring voids. The mean of the distribution is 3.3. The void size is 3. Material porosities are (a) 30% and (b) 40%.

Fig. 8 Effective Young's modulus vs. the standard deviation σ of the normal distribution for void size. The average void side length $\mu = 3$. Material porosities are (a) 30% and (b) 40%.

Fig. 9 Comparison with results presented in Refs. [5] and [6]

Fig. 10 Comparison with results presented in Ref. [10] and experimental results on powder sintered copper samples [13]

Figure 1

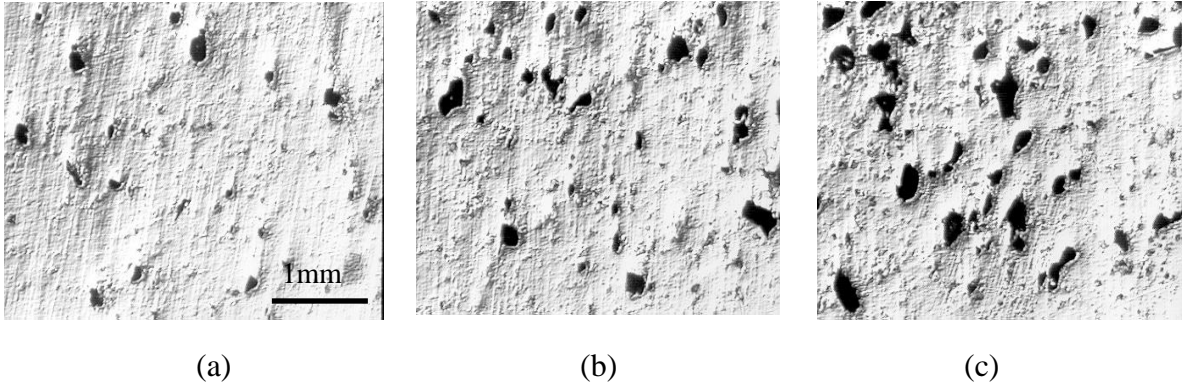


Figure 2

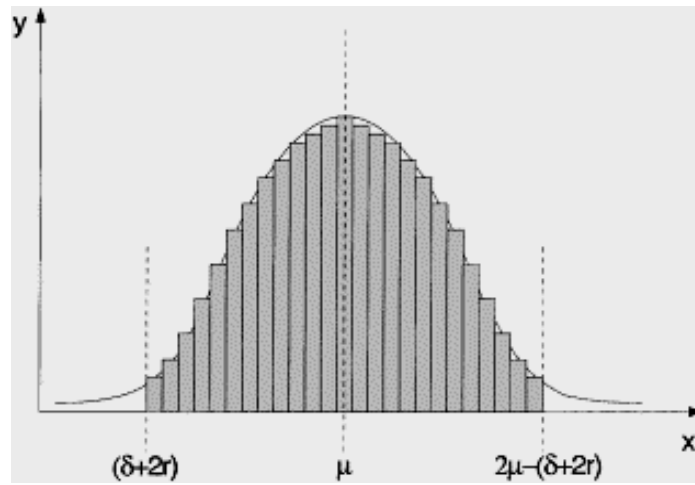


Figure 3

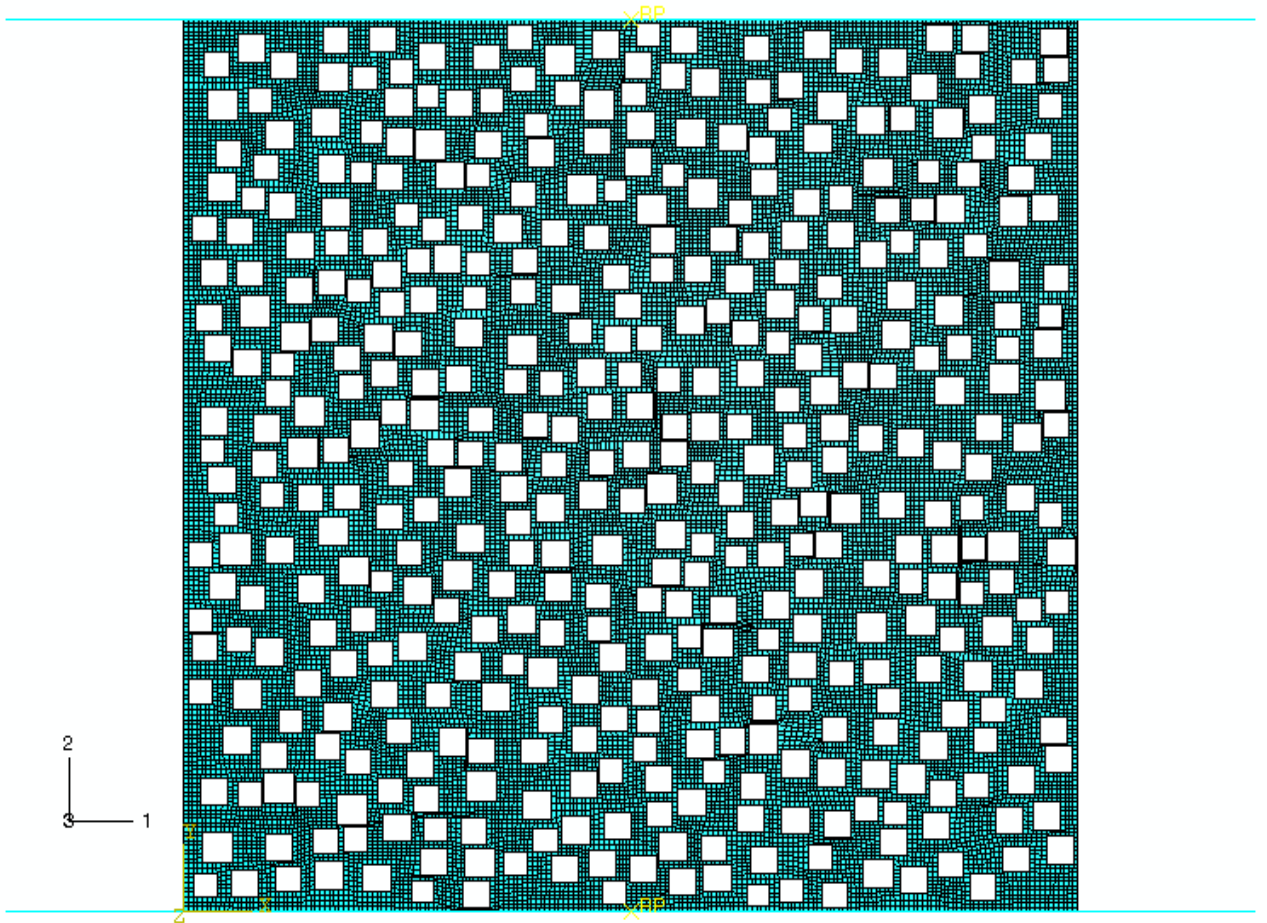


Figure 4

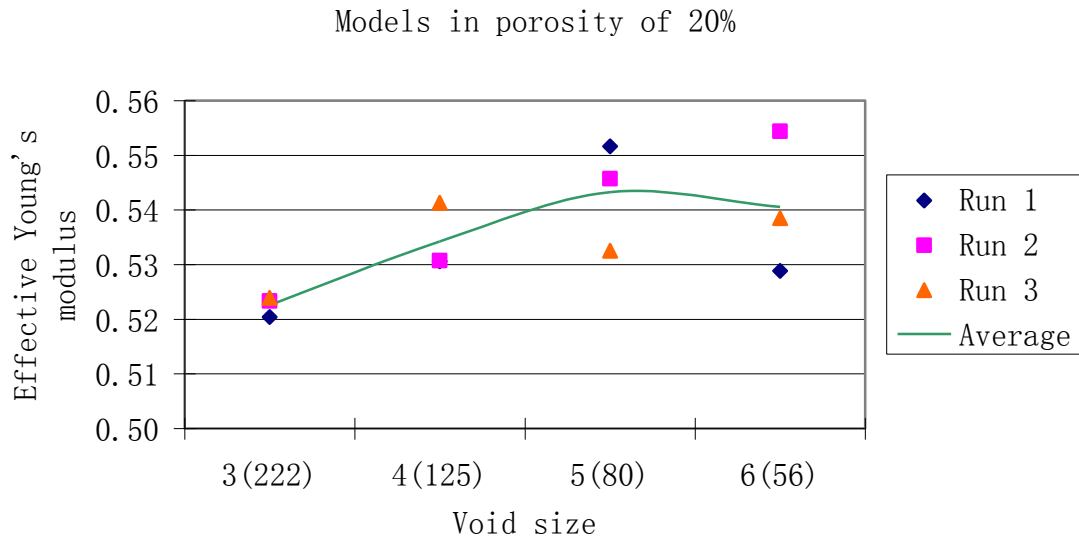


Fig. 4(a)

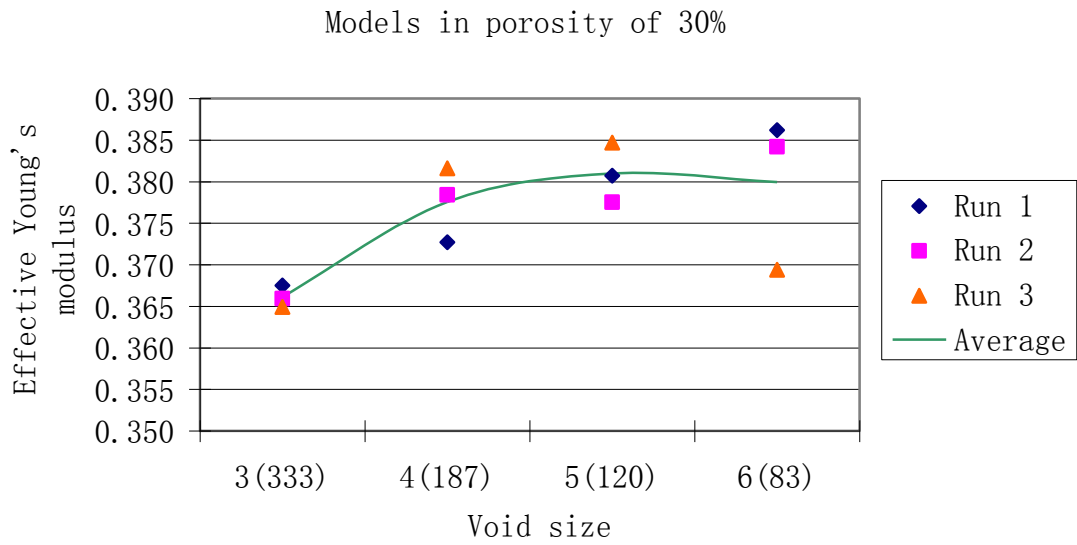


Fig. 4(b)

Figure 4 (continued)

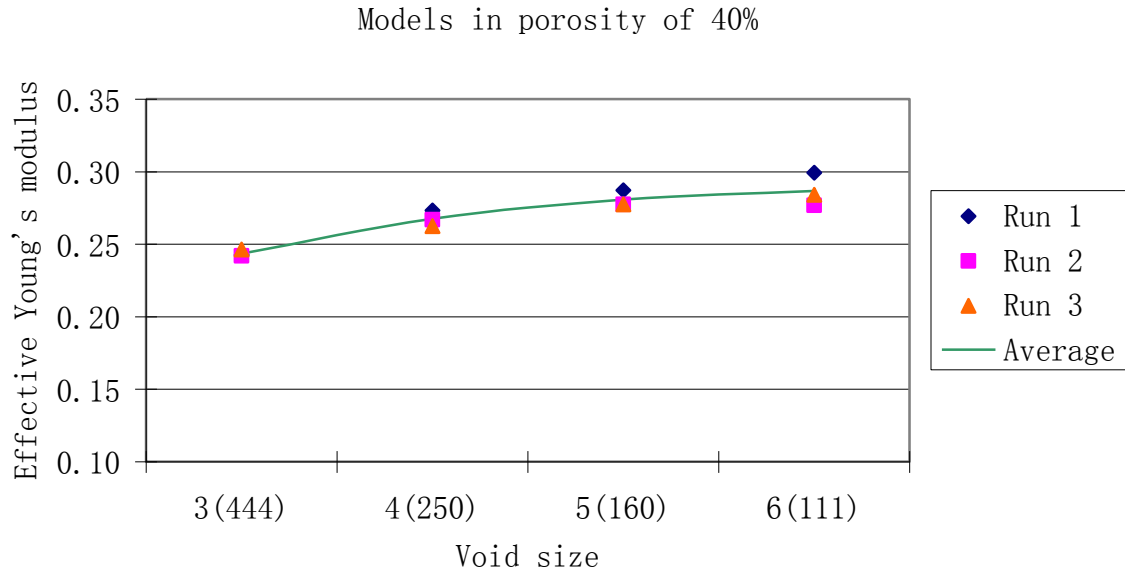


Fig. 4(c)

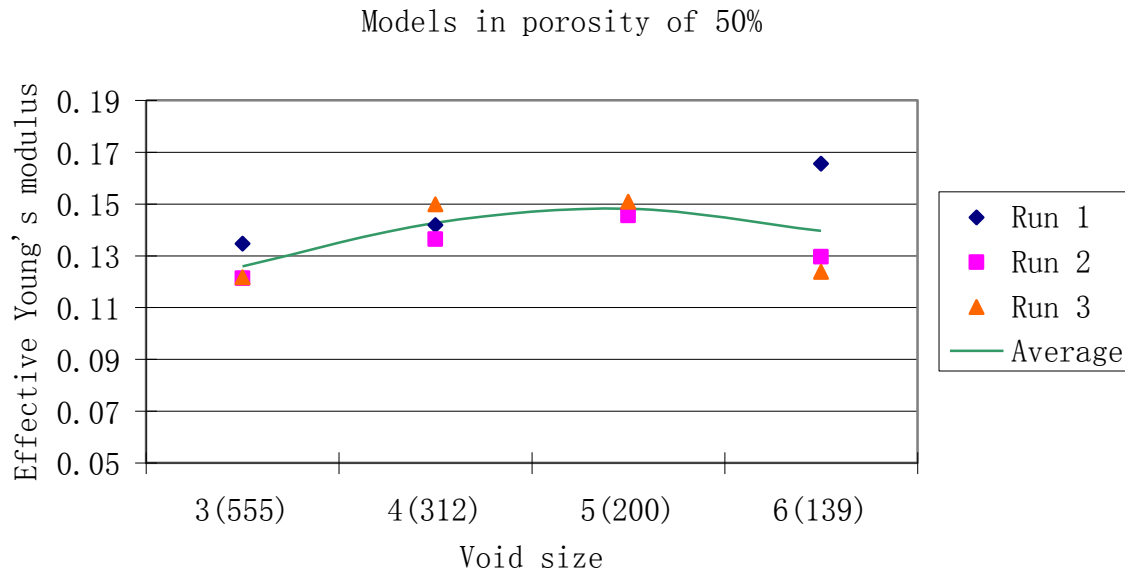


Fig. 4(d)

Figure 4 (continued)

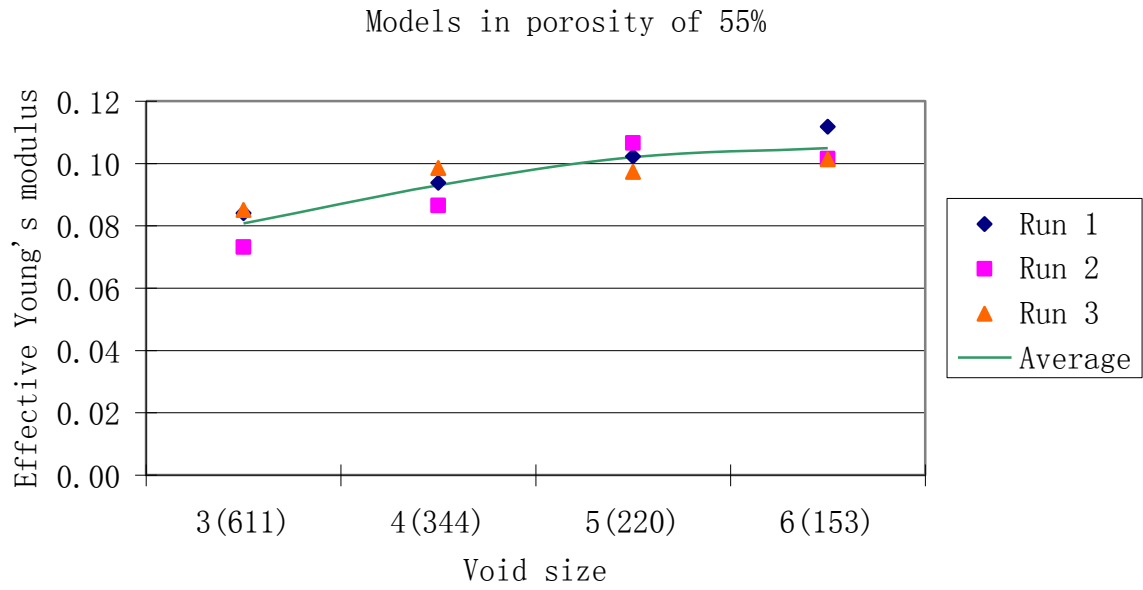


Fig. 4(e)

Figure 5

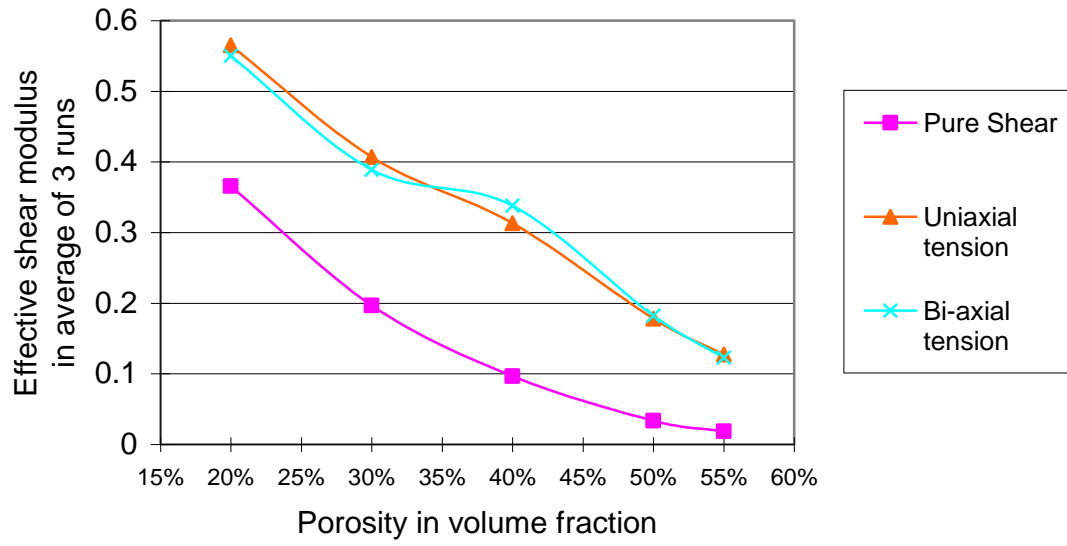


Figure 6

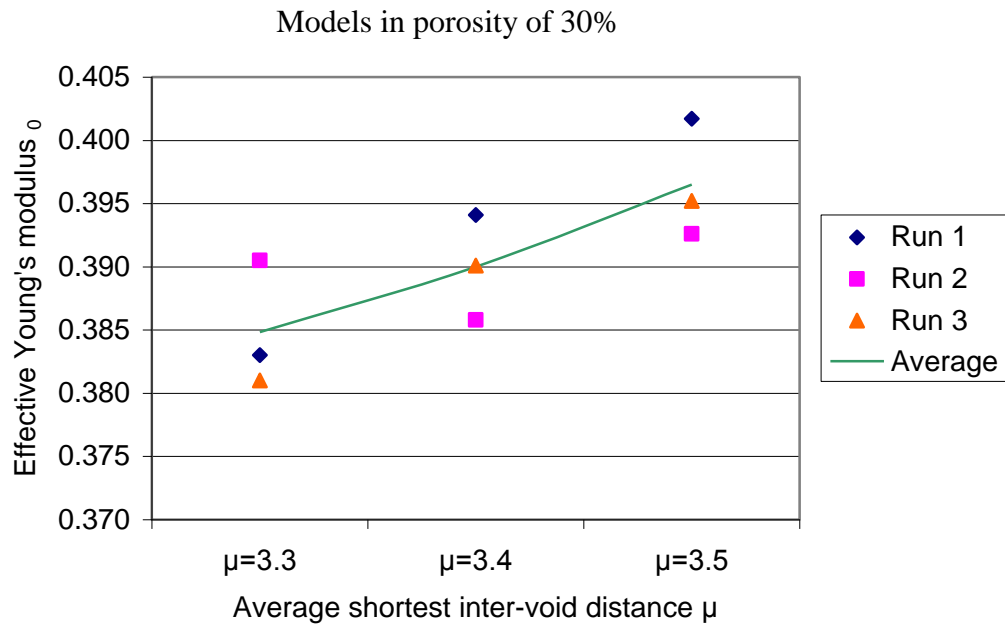


Fig 6(a)

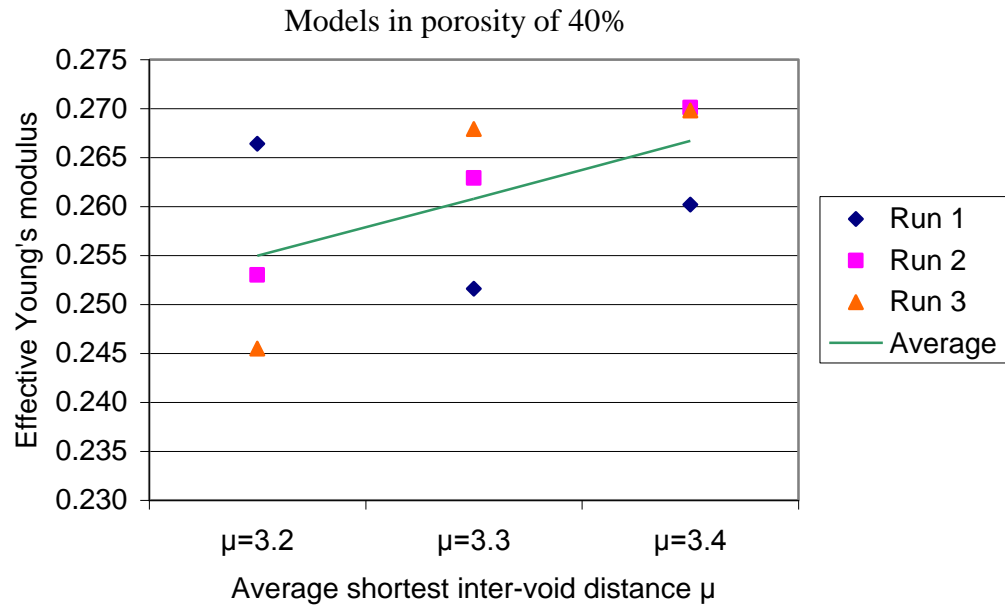


Fig 6(b)

Figure 7

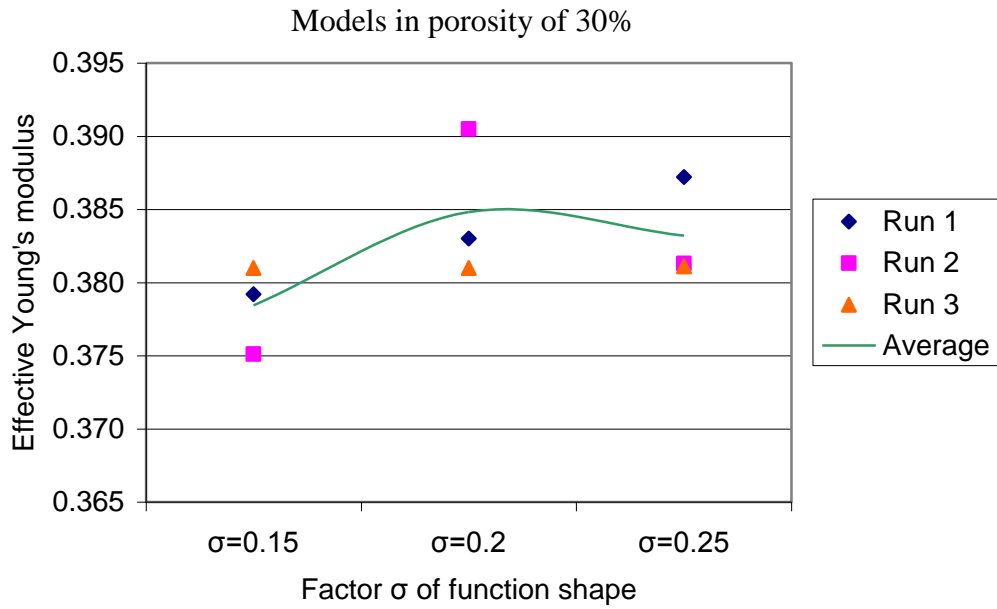


Fig 7(a)

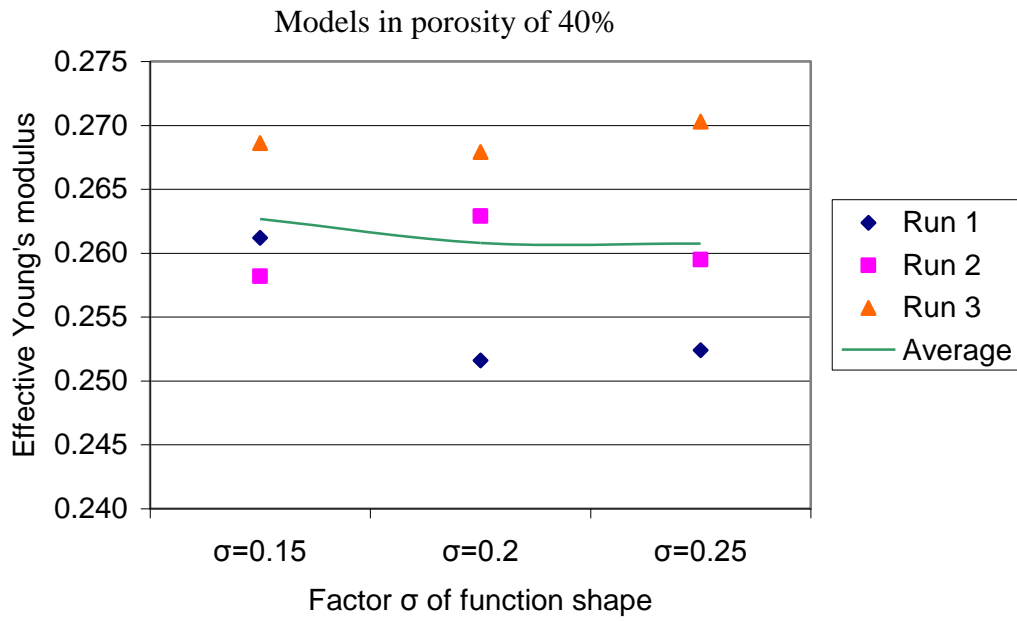


Fig 7(b)

Figure 8

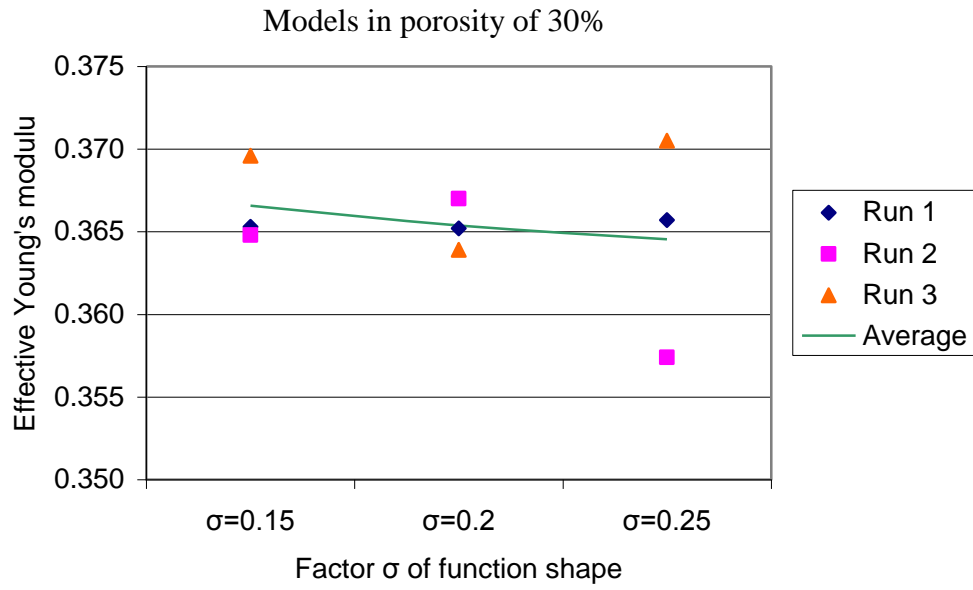


Fig 8(a)

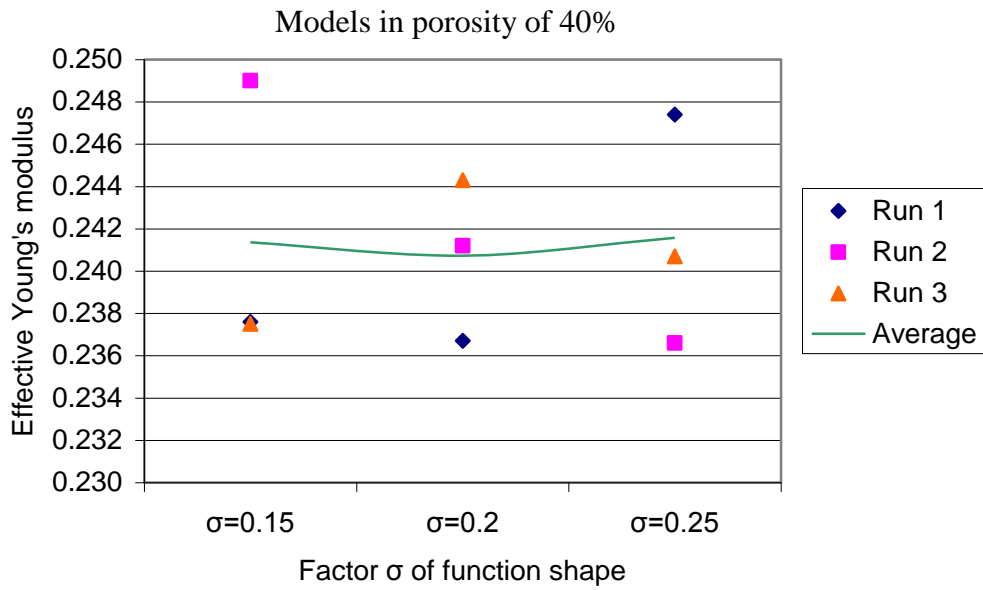


Fig 8(b)

Figure 9

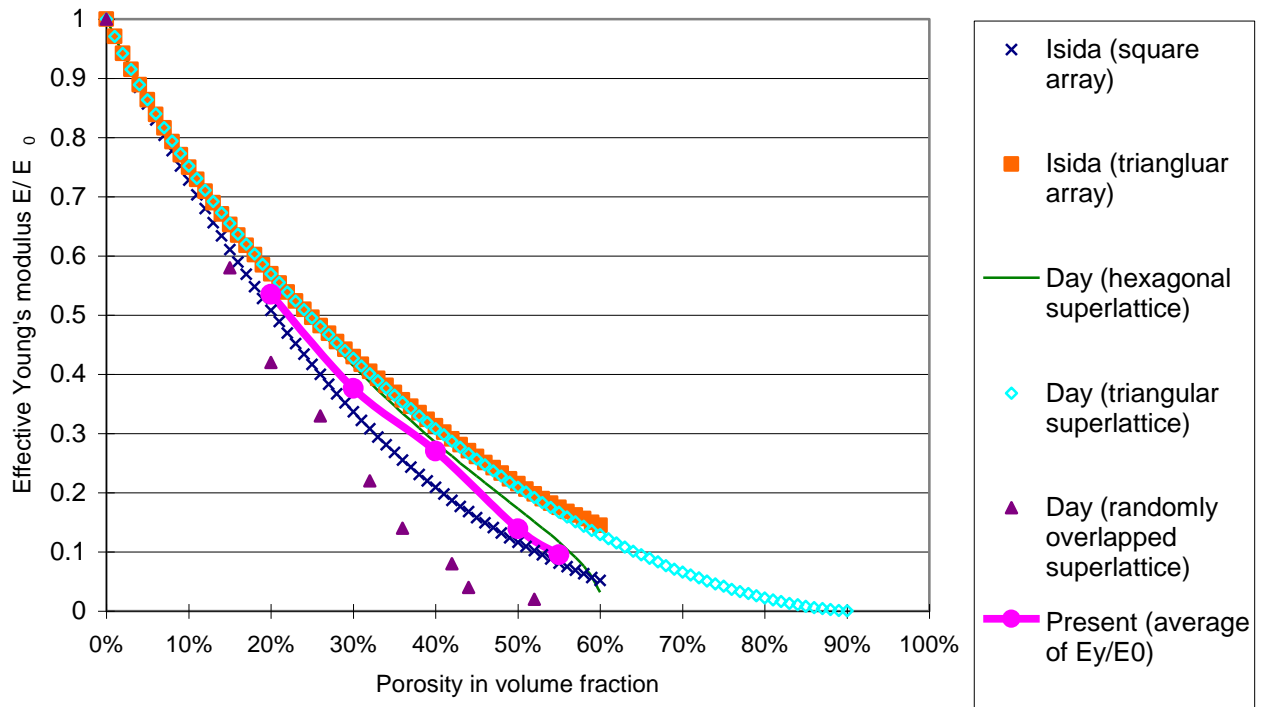


Fig. 10

